Appl Microbiol Biotechnol (2016) 100:3489–3498
DOI 10.1007/s00253-015-7193-x

Pilot-scale verification of maximum tolerable hydrodynamic stress for mammalian cell culture

Benjamin Neunstoecklin[1] · **Thomas K. Villiger**[1] · **Eric Lucas**[2] · **Matthieu Stettler**[2] · **Hervé Broly**[2] · **Massimo Morbidelli**[1] · **Miroslav Soos**[1,3]

Received: 18 September 2015 / Revised: 17 November 2015 / Accepted: 20 November 2015 / Published online: 5 December 2015
© Springer-Verlag Berlin Heidelberg 2015

Abstract Although several scaling bioreactor models of mammalian cell cultures are suggested and described in the literature, they mostly lack a significant validation at pilot or manufacturing scale. The aim of this study is to validate an oscillating hydrodynamic stress loop system developed earlier by our group for the evaluation of the maximum operating range for stirring, based on a maximum tolerable hydrodynamic stress. A 300-L pilot-scale bioreactor for cultivation of a Sp2/0 cell line was used for this purpose. Prior to cultivations, a stress-sensitive particulate system was applied to determine the stress values generated by stirring and sparging. Pilot-scale data, collected from 7- to 28-Pa maximum stress conditions, were compared with data from classical 3-L cultivations and cultivations from the oscillating stress loop system. Results for the growth behavior, analyzed metabolites, productivity, and product quality showed a dependency on the different environmental stress conditions but not on reactor size. Pilot-scale conditions were very similar to those generated in the oscillating stress loop model confirming its predictive capability, including conditions at the edge of failure.

Keywords Pilot scale · Mammalian cell culture · Maximum tolerable hydrodynamic stress · Downscaling · Upscaling

Electronic supplementary material The online version of this article (doi:10.1007/s00253-015-7193-x) contains supplementary material, which is available to authorized users.

✉ Massimo Morbidelli
massimo.morbidelli@chem.ethz.ch

✉ Miroslav Soos
miroslav.soos@chem.ethz.ch

[1] Department of Chemistry and Applied Biosciences, Institute for Chemical and Bioengineering, ETH Zurich, 8093 Zurich, Switzerland

[2] Merck Serono S.A., Biotech Process Sciences, Corsier-sur-Vevey, Switzerland

[3] Department of Chemical Engineering, University of Chemistry and Technology, Technicka 3, 16628 Prague, Czech Republic

Introduction

Bioprocess scale-up in cell culture industry is a task often still based more on historical experience rather than on scientific knowledge. Differences in process performance are commonly observed in-between scales which result from intrinsic differences between laboratory and production scales (Humphrey 1998; Mostafa and Gu 2003; Li et al. 2006; Yang et al. 2007; Xing et al. 2009). Classical scaling rules suggested to keep various reactor characteristics such as power input or tip speed constant (Glacken et al. 1983; Ju and Chase 1992; Marks 2003; Nienow 2006). However, these criteria are not satisfactory and often provide contradicting results (Schmidt 2005). Further complication comes from the determination of the maximum values for the shear rate or the hydrodynamic stress tolerated by cells.

Pioneering works in bubble-free systems with classical single-vessel bioreactors were conducted by Oh et al. (1989) reporting an agitation tip speed (v_{tip}) of 1.4 m/s, corresponding to a power input of 1.9×10^{-1} W/kg, to ensure no cell damage. In contrast, Leist et al. (1986) report tip speeds of 3.5 m/s (1.5 W/kg) and Kunas and Papoutsakis (1990) of 2.6 m/s (2.7 W/kg) to be safe for cell culture, while Al-Rubeai et al. (1995) report of 1.9 m/s (3.1×10^{-1} W/kg) to be above the cell damage threshold. This wide range of proposed values is further enlarged by the presence of bubbles. Under multiphase

conditions and without the presence of shear protective agents, such as Pluronic F-68, critical tip speeds around 0.5 m/s (3.3×10^{-2} W/kg) and maximum gas flow rates between 0.02 and 0.03 vvm have been reported in the literature (Oh et al. 1992; Cruz et al. 1998). Although the addition of Pluronic can minimize the detrimental effects of bubbles (Murhammer and Goochee 1990; Chalmers and Bavarian 1991; Jöbses et al. 1991; Oh et al. 1992; Ma et al. 2004). it results in a reduction of mass transfer (Murhammer and Pfalzgraf 1992; Sieblist et al. 2013) leading to higher stirring speeds required to meet the oxygen demand and CO_2 removal. Therefore, the knowledge of the maximum hydrodynamic stress tolerated by cells is an essential piece of information, which has to be known during process scale-up and optimization. While in the case of weak cells classical single-vessel bioreactors can be readily used to obtain this quantity, in the case of particularly robust cells the specific stress threshold cannot be resolved using classical single-vessel bioreactors. Typically, this is due to equipment limitations or vortex formation resulting in bubble entrapment and foam formation. In addition, the above mentioned approaches do not address the heterogeneous nature of multiple parameters present in large-scale reactors, i.e., spatial variations in stress (Soos et al. 2013). pH (Osman et al. 2002). and gaseous compositions (Amanullah et al. 1993; Serrato et al. 2004).

In a stirred vessel, cells are subject to an oscillating hydrodynamic stress as they travel from the quiet region far from the impeller to the highly turbulent one close to it. This can be simulated by the laminar extensional flow device developed by the group of Chalmers (Ma et al. 2002; Mollet et al. 2007; Godoy-Silva et al. 2009a, b). Here the culture broth was forced through an external loop equipped with a well-defined nozzle, exposing the cells to laminar stress values ranging from 1.2×10^{-2} to 6.4×10^{3} W/kg. However, due to the operating procedure, this device cannot fully decouple exposure frequency and exposure duration, therefore limiting its capability to mimic the stress history experienced by cells in differently scaled vessels. Additionally, as discussed by Nienow et al. (Nienow 2006; Nienow et al. 2013). the use of laminar flow conditions represents an intrinsic limitation when considering manufacturing-scale bioreactors, which typically operate in highly turbulent conditions.

More recently, two different procedures using lab-scale bioreactors have been proposed to address this issue. The first one is based on the application of constant high average power input in a turbulent single-vessel stirred bioreactor. This approach exposes cells to high hydrodynamic stress at a higher frequencies compared to large-scale reactors (Nienow et al. 2013). The second strategy developed by Sieck et al. (2013) tries to align the frequency of high stress values to mimic the change from high to low hydrodynamic stress, but still the range of possible stresses experienced at the manufacturing scale remains larger. In order to employ turbulent flow conditions and decouple exposure period and hydrodynamic stress magnitude, Neunstoecklin et al. (2015) recently proposed a scale-down model, where a 3-L bioreactor is equipped with an external loop capable of generating a broad range of hydrodynamic stresses (15 to 103 Pa). This system was used to determine the stress threshold values for a Sp2/0 and a CHO cell line using a fed-batch cultivation process.

Although this quantity is of high industrial importance during process scale-up, no systematic study exists in the open literature where the cell response measured in small scale is compared with a large-scale cultivation system operated beyond or at the edge of failure. Therefore, the main goal of this work is to provide such a comparison and validation of a scale-down model. In this study, stress values below as well as above the previously measured threshold for the Sp2/0 cells (Neunstoecklin et al. 2015) have been applied using a 300-L pilot-scale bioreactor. Prior to cultivation, the maximum hydrodynamic stress was characterized using a shear-sensitive particulate system (Villiger et al. 2015). Measured growth behavior, metabolism, productivity, and critical quality attributes were compared to historical data measured in the oscillating hydrodynamic stress loop model.

Materials and methods

Bioreactor setup

A pilot-scale bioreactor with a working volume of 300 L (New MBR, Switzerland) equipped with four baffles and a combination of Rushton and marine impeller was used. The Rushton impeller was mounted at the bottom of the vessel, while the marine impeller was mounted at a higher elevation on the same shaft pumping the liquid upward. Geometric details of the compared reactor scales are given in Fig. 1a. The key reactor operating parameters are compared in Table 1. Calculation of the volume average energy dissipation rate of the used bioreactor was performed as follows (Perry et al. 1997):

$$\langle\varepsilon\rangle = \frac{N_p D^5 N^3}{V} \quad (1)$$

where N_p is the power number of the impeller, D is the impeller diameter (m), N is the agitation rate (1/s), and V is the bioreactor volume (m^3). Impeller Reynolds numbers are reported in Table 1 to verify turbulent conditions. Two selected cultivation conditions were used to expose cells to stress values well below and above the previously determined threshold value of 25 Pa for those cells (Neunstoecklin et al. 2015). Cultivation results obtained from the 300-L bioreactor are compared with those measured previously (Neunstoecklin et al. 2015) using a 3-L bioreactor equipped with an external loop as shown in Fig. 1b.

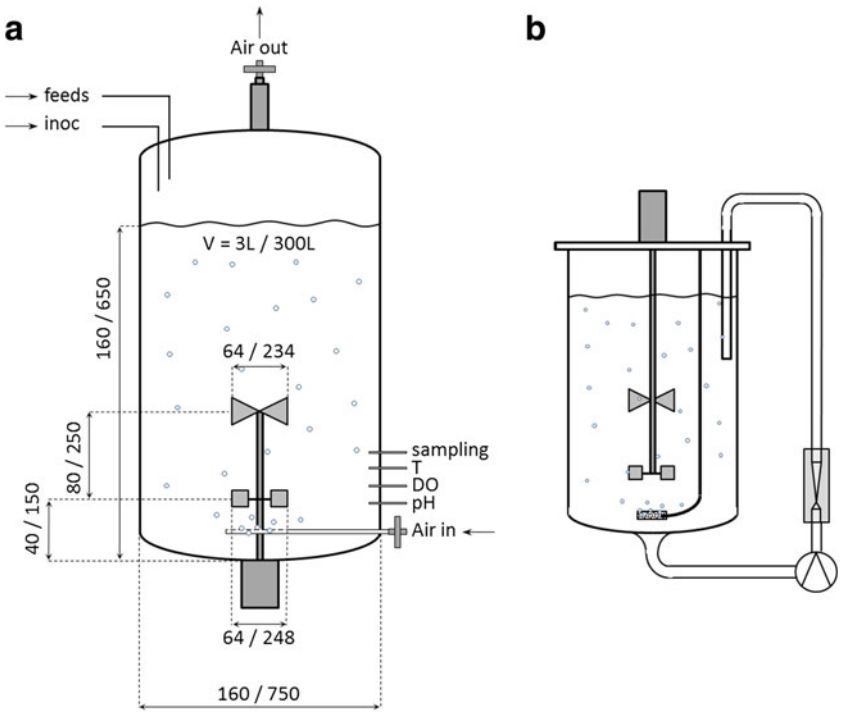

Fig. 1 In (**a**), the dimensions of the bioreactors considered in this study are given. Values refer to bioreactors with a volume equal to 3 and 300 L, respectively (all values in millimeters). In (**b**), the shear loop model described by Neunstoecklin et al. (2015) and used to generate high oscillating stress at small scale is shown

Hydrodynamic stress characterization

The maximum hydrodynamic stress values (τ_{max}) in the bioreactors were determined using a procedure developed by Villiger et al. (2015). This procedure is based on the measurement of the maximum stable size of aggregates composed out of polymeric nanoparticles. When exposed to certain hydrodynamic stress, these aggregates undergo breakup until steady state size, which is controlled by the maximum stress present in the system (Soos et al. 2008, 2013; Ehrl et al. 2010). Although the size of these aggregates is comparable to the size of mammalian cells, the obtained stress values may only be indicative of the stress to which cells are exposed to during the cultivation process, yet this scalable measurement allows quantifying the highest stresses between different scales and equipment. A detailed description of the method can be found in the original work of Villiger et al. (2015).

Cell line and inoculum preparation

The cell line used in this study was derived from a Sp2/0 host cell line producing a commercialized monoclonal antibody. A cell bank vial was directly thawed into complex proprietary media for the expansion of cells. Density after thawing was $0.5 \pm 0.1 \times 10^6$ cells/mL, and subcultivation of the cells was performed every other day to keep the cell density below $1.5 \pm 0.1 \times 10^6$ cells/mL. Initially, orbitally shaken T-flasks were used, and after reaching an appropriate volume, the cells were transferred in glass spinner flasks (Integra, Switzerland) and cultivated at 37 °C with 90 % humidity. Spinner flasks were aerated through an open pipe sparger using air supplemented with 5 % CO_2. Duration of the expansion was always 29 days, after which cells were used for inoculation. Each experiment was inoculated with freshly prepared inoculum culture, and seeding was performed into a prefilled bioreactor using the same media, with a target cell density of 0.3×10^6 cells/mL.

Cell cultivation and offline data analysis

The 300-L bioreactor was controlled at an agitation speed of 71 rpm and a DO set point of 60 % air saturation. The latter was first controlled with air until a flow rate of 0.4 L/min was reached. After this point, oxygen was added to the gas stream on demand resulting in maximum total volumetric gas flow

Table 1 Operating conditions for the bioreactor cultivations

V_{Bio} (L)	N (rpm)	D (m)	v_{tip} (m/s)	N_p (−)	Re_{Imp} (−)	$<\varepsilon>$ (W/kg)	τ_{max} (Pa)
3	110	0.06	0.346	5.4	9474	8.6×10^{-3}	1.2
300	71	0.23	0.855	5.4	89,856	1.9×10^{-2}	7
300	150	0.23	1.806	5.4	189,838	1.8×10^{-1}	28

rate of 2 L/min, corresponding to 0.0067 vvm. The effect on the corresponding power input was neglected due to the low gas flow rate (Nienow 1998). The overall power number for the two mounted impellers was assumed to be equal to the sum of the individual ones (Hudcova et al. 1989). i.e., 5.0 for the Rushton turbine (Perry et al. 1997) and 0.4 for the up-pumping marine impeller (Paul et al. 2003). giving a total of 5.4. With an agitation speed of 71 rpm, this results in an $\langle\varepsilon\rangle$ of 1.9×10^{-2} W/kg with τ_{max} being equal to 7 Pa. To investigate stress values beyond the threshold, this reactor was operated in a second experiment at an agitation speed of 150 rpm corresponding to $\langle\varepsilon\rangle$ equal to 1.8×10^{-1} W/kg with τ_{max} equal to 28 Pa. The pH was controlled via CO_2 with a set point of 7.1 until day 3 when a step change down to 6.9 was applied. This value was kept constant for the rest of the process. A concentrated nutritional bolus feed was added when a cell density of 2×10^6 cells/mL was reached, usually occurring on day 2 or 3, containing a complex mixture of glucose, amino acids, and proteins.

Daily samples were taken from all cultures to follow the growth behavior and the production and consumption of nutrients and metabolic products. The samples were used to monitor cell density and viability (Vi-CELL, Beckman Coulter, USA), pH (SevenMulti, Mettler-Toledo, Germany), pO_2 and pCO_2 (ABL5 blood gas analyzer, Radiometer, Switzerland), metabolites (Nova CRT, Nova Biomedical, USA), turbidity (Turb 550, WTW, Germany), and osmolality (Micro Osmometer, Advanced Instruments, USA). The amount of produced protein was analyzed by standard HPLC analysis using protein A. Product quality was analyzed after protein A capture by size exclusion chromatography for protein aggregates (Berridge et al. 2009). Glycosylation analysis was performed via gel electrophoresis (CGE-LIF) using the procedures developed by Papac et al. (1998) and Rapp et al. (2011). Charged variants were analyzed via capillary isoelectric focusing (cIEF) using an iCE280 system (ProteinSimple, USA).

Specific consumption and production rates were calculated as follows:

$$q_i = \frac{\Delta c_i \cdot 2}{\Delta t (X_t + X_{t+1})} \quad (2)$$

where q_i is the specific metabolic rate, Δc_i is the concentration difference of the corresponding metabolite, Δt is the time difference in between two consecutive culture samples, and x is the viable cell density (Adams et al. 2007).

Results

Shear characterization of the pilot-scale bioreactor

When using stirred and sparged bioreactors, the cell culture broth is exposed to various sources of hydrodynamic stress originating from turbulent flow, gas jet present during bubble formation, bubble rise, or bubble burst (Oh et al. 1992; Michaels et al. 1996; Cruz et al. 1998; Chisti 2000; Zhu et al. 2008; Liu et al. 2013; Villiger et al. 2015). To evaluate the relative contribution of stirring and sparging to the maximum hydrodynamic stress present in a 300-L bioreactor, this was characterized by the shear sensitive system developed by Villiger et al. (2015). Effects from bubble burst were eliminated by the use of Pluronic F-68 at the same concentration as used for subsequent culture experiments (Boulton-Stone and Blake 1993; Jordan et al. 1994; Clincke et al. 2010; Villiger et al. 2015). The advantage of this characterization system is its capability to describe the experienced by the cells in any system independent on its scale, shape, or material (see Supplementary Fig. S1). This makes it possible to compare stainless steel and single-use devices including non-stirred-based systems like wave-rocking bioreactors or shake flasks.

In order to determine the relative importance of the above mentioned mechanisms, τ_{max} was measured for various combinations of stirring and sparging for the 300-L bioreactor. Two types of ring spargers, which were located below the Rushton impeller, were equipped with either eight sintered spargers (average pore diameter equal to 50 μm) or eight nozzles with a diameter of 1 mm. The obtained results are shown in Fig. 2. The maximum hydrodynamic stress for non-aerated conditions monotonically increases with Re_{Imp}. When considering intermediate gas flow rates, corresponding to 0.03 vvm, values of τ_{max} measured for the sinter sparger are very similar to those measured for single-phase conditions, indicating negligible contribution of small bubbles. In contrast, when openings with 1-mm diameter were used, generating larger bubbles, the value of τ_{max} increases at low Re_{Imp}, to about 5 Pa with gas flow rates of 0.03 vvm and about 8 Pa for 0.09 vvm (see Fig. 2). By further increase of Re_{Imp}, this effect

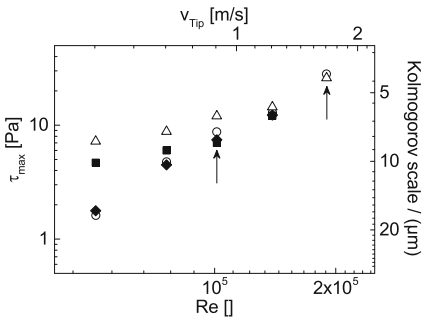

Fig. 2 Maximum hydrodynamic stress, in a 300-L bioreactor measured by the shear-sensitive particulate system developed by Villiger et al. (2015). Two types of spargers, one with a hole opening of 1 mm and the other with a 50-μm sinter sparger, were investigated combining various agitation speeds and gas flow rates. *Open circles* correspond to the non-aerated single-phase condition. The applied gas flow rates, for an open pipe sparger with a hole opening of 1 mm, were equal to 0.03 vvm (*filled square*) and 0.09 vvm (*open triangle*), while for 50-μm sparger, only gas flow rate equal to 0.03 vvm (*filled diamond*) was analyzed. *Arrows* indicate the conditions used for the cell culture experiments

becomes negligible indicating that at high Re_{Imp}, the maximum hydrodynamic stress is dominated by the turbulence generated by the impeller. Arrows in Fig. 2 indicate the two cultivation conditions used, applying maximum gas flows of 0.03 vvm using sintered spargers. As can be seen from Fig. 2 in both cultivation conditions, the maximum hydrodynamic stress originates from stirring with negligible effect of sparging. For completeness, the same analysis was done for the 3-L bioreactor (see Supplementary Fig. S2). A more detailed discussion on these results can be found in the original article (Neunstoecklin et al. 2015). Moreover, in all cultivations, the effect of bubble burst was prevented, through the use of Pluronic F-68, which is known to inhibit the attachment of cells to bubbles (Handa-Corrigan et al. 1989; Trinh et al. 1994; Wu 1995; Meier et al. 1999; Gigout et al. 2008). A commonly used parameter to assess cell damage caused by mixing phenomena is the Kolmogorov's microscale, η, which is a function of the ratio between the turbulence intensity (represented by the local EDR, ε) and the kinematic viscosity of the liquid (ν) given as $\eta=(\nu^3/\varepsilon)^{1/4}$. It has been proposed that cell damage occurs when the eddy diameter η reaches the size of a freely suspended cell (Croughan et al. 1987; Oh et al. 1989; Chisti 2000; Flickinger 2013). The measured maximum stress values were recalculated ($\varepsilon=\tau^2/\rho\mu$) and expressed as the corresponding Kolmogorov scales with illustrative purpose in Fig. 2. As can be seen from the two cultivation conditions indicated with arrows and performed at 71 rpm (≈90,000) and 150 rpm (≈190,000), the size of the smallest eddies is equal to 8 and 4 μm, respectively. On the other hand, when calculating the mean Kolmogorov length scale based on the vessel averaged energy dissipation rate using the whole vessel volume, sizes are 65 and 37 μm, respectively. With an average cell size of 15 μm, cell damage would be expected for both conditions regarding local quantities but not for the averaged ones. Because reduced growth was observed for the culture with higher agitation but not for the other, we conclude that the use of the Kolmogorov scale cannot discriminate in between the two applied conditions and suggest the use of an experimentally derived maximum stress as presented by Villiger et al. (2015).

Proliferation behavior of the cells

Prior to this study, the described SP2/0 cell line was characterized upon its hydrodynamic stress resistance using a specially designed shear loop system (Neunstoecklin et al. 2015). It was found that for the studied cells, the threshold is equal to 25.2±2.4 Pa. It is worth noting that an alternative to the applied loop system would have been the use of a single bioreactor, operated under elevated stirring speed and thus resulting in higher stresses (Nienow et al. 2013). However, due to the robustness of the studied industrial cell line, the very high stirring speeds required was above the maximum operating limit of the motor. Furthermore, even before reaching the maximum stirring speed, the formation of vortexes was observed resulting in a non-desired secondary effect of bubble entrapment and consequent breakup (Kunas and Papoutsakis 1990; Hua et al. 1993; Emery et al. 1995; Chisti 2000).

To validate the proposed shear loop system, the same SP2/0 cell line was cultivated at conditions below and above the stress threshold, using a 300-L pilot-scale vessel. In particular, cultivations were performed at 71 rpm (≈90,000) corresponding to a stress of 7 Pa being well below the threshold and at the maximum agitation speed possible for the given reactor which is 150 rpm (≈190,000) corresponding to 28 Pa (see Fig. 2). Vortex formation was not observed at any conditions, due to the upward pumping marine impeller. In order to compensate for run-to-run variabilities all data were aligned to the time point of the initial bolus feed, performed after reaching a cell density of 2×10^6 cells/mL, as described in the "Materials and methods" section. To identify differences between cultivations performed at different stresses and scales, data were analyzed using Student's paired two-sample t test. Hence, p values above 0.1 where considered as equivalent to the control culture and p values below 0.1 were considered as different, while values lower than 0.05 were considered as significantly different. The growth profiles of 300-L cultures together with published data (Neunstoecklin et al. 2015) obtained from either 3-L cultivations in classical single vessels, applying stress values of 1.2 Pa, or 3-L systems equipped with an external loop generating maximum stress values of 21 or 38 Pa are compared in Fig. 3a. In the case of low stress, the measured data in the 300-L bioreactor closely follows the growth and viability profile of the 3-L system at 1.2 Pa (Fig. 3a, b) with an exception on day 5 where the 300-L culture shows a higher cell density. This aligned trend is furthermore valid for the integral viable cells (IVC) and the cell aggregates in the culture (Fig. 3c, d). Furthermore, results are very alike when comparing the data from the 300-L run at 28 Pa with the 3-L oscillating shear model applying 21 Pa. For both, the maximum cell density decreases from 5×10^6 down to 4×10^6 cells/mL and the viability profile is first comparable with the standard but stays higher after day 7. The cellular aggregation rate is significantly reduced with p values below 0.05, in particular observed between days 2 and 7, thus confirming the higher hydrodynamic stress values present in both systems.

Cell metabolism and productivity

Cell culture samples were measured daily for glucose (GLC), lactate (LAC), glutamine (GLN), glutamate (GLU), and ammonia (NH4) as described in the "Materials and Methods" section. From the obtained values, specific rates were calculated according to Eq. (2). As can be seen from Supplementary Fig. S4, no significant difference of specific rates was observed between the applied conditions. With lactate being

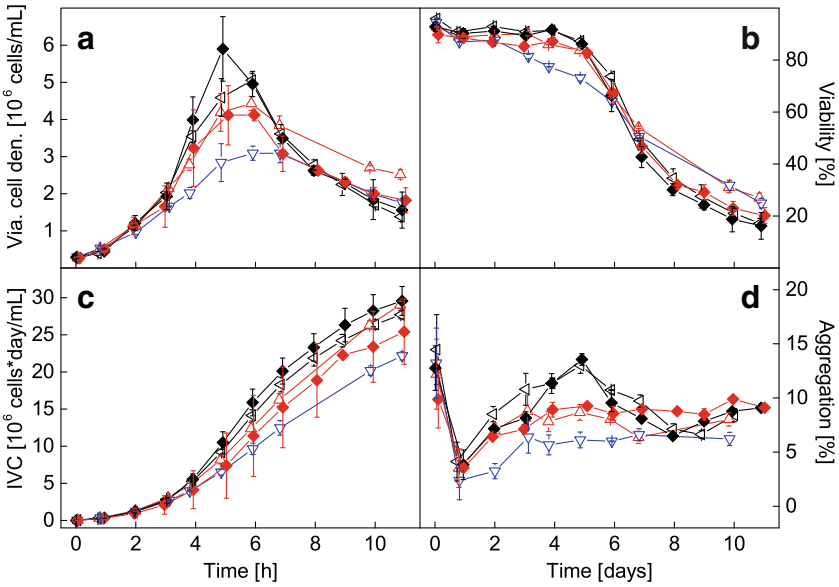

Fig. 3 Comparison of the growth behavior (**a**, **b**, **c**) and the morphology (**d**) of the Sp2/0 cell line cultured in 300-L bioreactors using maximum stress values of 7 Pa (*black diamond*) and 28 Pa (*red diamond*), together with data measured in 3-L scale using maximum stress values of 1.2 Pa (*black triangle*), 21 Pa (*red triangle*), and 38 Pa (*blue triangle*) (Neunstoecklin et al. 2015). *Error bars* represent 1 standard deviation and are obtained from at least two independent cultivations. Statistical analysis, based on Student's paired two-sample *t* test, is provided in the text (Color figure online)

one of the most important metabolite stress indicators, usually used to interpret the well-being of the culture (Li et al. 2010, 2012; Zagari et al. 2012; Le et al. 2012). it can be seen in Fig. 4a that lactate concentrations are significantly lower with p values below 0.05 for cultures with higher stress values, accompanied with lower growth, resulting in specific rates that are very similar. The cumulative amount of glucose shown in Fig. 4b gives a good picture on the energy metabolism of the cells where cultures applying higher stress in both scales consume significantly lower amounts of glucose ($p<0.05$). This goes along with the lower growth and lactate production described before. Additionally, the specific productivity shows a decreasing trend from values around 37 to 10 pg/cell/day, when conditions beyond the threshold of 25.2 ±2.4 Pa were applied (Supplementary Fig. S3b). Apart from the culture with 38 Pa which was vastly over the cell line threshold, this can also be observed in Fig. 4c where the total amount of product at the day of harvest is the lowest ($p>0.05$), for the 300-L experiment performed at 28 Pa. Interestingly, highest titers could be observed for the conditions applying 21 Pa in the 3-L system with about 15 % more final product than obtained for the control culture. Here the paired t test resulted in a p value of 0.5 indicating no difference between the experiments, declared by the aligned titer profile for the first 8 days. The final titer increase can be explained by the increased longevity of this culture with an approximately 10 % higher viability from day 6 on compared to the control. Similar findings are reported by Senger and Karim (2003) who realized increased production of total recombinant tissue-type plasminogen activator protein when applying moderate shear. These findings indicate the possibility, to increase productivity through hydrodynamic stress, as long as the critical threshold is not exceeded.

Effect on key product quality attributes

Several authors discussed the effect of laminar or turbulent flow on the behavior of mammalian cells during culture and their effect on the final product. Particular attention is paid to the influence on the quality of the protein. Most reports conclude that only minor effects on quality attributes like glycosylation or charged variant distribution are found as long as no change in the growth behavior and the basic metabolite can be observed (Senger and Karim 2003; Scott et al. 2012; Sieck et al. 2013; Nienow et al. 2013; Neunstoecklin et al. 2015). Only one study exists that claims to observe significant changes in the glycosylation at hydrodynamic conditions below the threshold affecting growth and metabolism (Godoy-Silva et al. 2009a).

In this work, we found that the effect of hydrodynamic stress on the measured quality attributes (nine major glycoforms) for sublethal conditions is negligible (Fig. 5a). It can be seen that for conditions below the threshold (black 1.2 Pa, forward slash 15 Pa, and back slash 7.8 Pa), independent on the vessel size, the distributions are very similar. Values above 25 Pa (vertical line 38 Pa and horizontal line 28 Pa) show a shift toward more complex glycan structures and in particular toward the bi-antennary form FA2G2aG2 (Fig. 5a, structure 8), being distinctly higher compared to the control. A very similar trend is visible for the charged variant profiles (Fig. 5b). For stress values below the threshold, only minor changes are observed, while increasing the stress above the threshold results in a distribution shift to the right, toward more alkaline forms. The distribution for both the glycosylation and charged variants depends on the applied hydrodynamic stress beyond the threshold, and not on the reactor size. This becomes clear when comparing the patterns of the 3-L

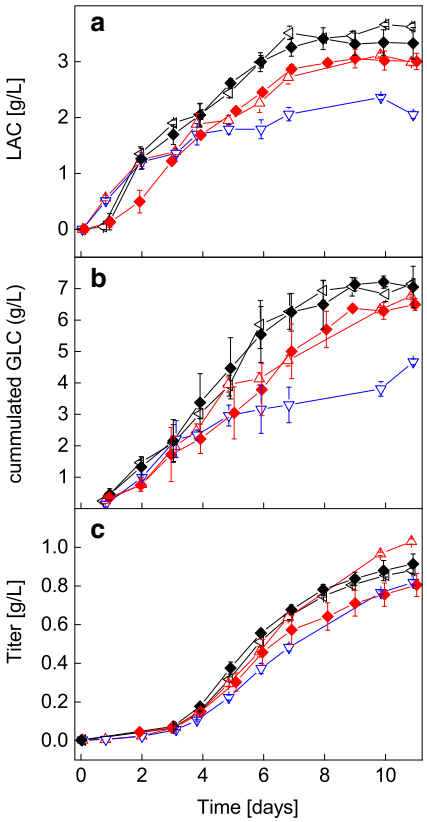

Fig. 4 Lactate (**a**) and product titer (**b**) production for the considered cultivations. Maximum stress values applied at 3 L were 1.2 Pa (*black triangle*), 21 Pa (*red triangle*), and 38 Pa (*blue triangle*) (Neunstoecklin et al. 2015). while at 300 L, they were 7 Pa (*black diamond*) and 28 Pa (*red diamond*). *Error bars* represent 1 standard deviation and are obtained from at least two independent cultivations. Statistical analysis, based on Student's paired two-sample *t* test, is provided in the text

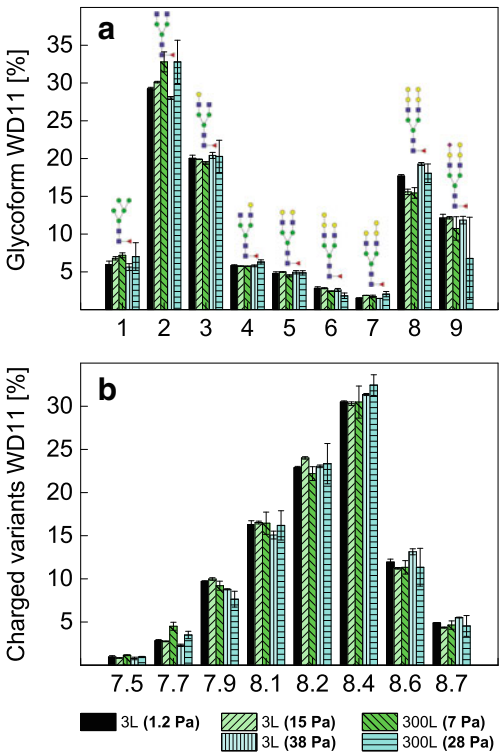

Fig. 5 Comparison of glycosylation (**a**) and charged variant (**b**) profiles at day 11 measured in 3-L and in 300-L bioreactors for various values of the maximum hydrodynamic stress. *Numbers* on the *x*-axis in (**a**) represent the nine separated glycoforms, shown with their antennary structure above the bars of the plot. The *x*-axis in (**b**) shows the isoelectric point of the corresponding charge variant. *Error bars* represent 1 standard deviation and are obtained from at least two independent cultivations

run at 15 Pa (forward slash) and the 300-L run at 7 Pa (back slash). Results in between the two are very similar. The same applies to the 3-L run at 38 Pa (vertical line) and the 300-L run at 28 Pa (horizontal line). Apart from the described trends, there was no statistical difference found between either scales or applied stresses with all p values being well above 0.1. Generally, the response to the applied operating condition, i.e., hydrodynamic stress, results in suboptimal growth and therefore in the same change in quality, which in reverse can be used as a fingerprint representing the operating conditions. In Supplementary Fig. S5, the glycosylation and charged variants profiles are displayed during late exponential phase at day 5. Absolute values at this day are different but the overall trends are the same as discussed above. These results indicate the strong dependency of quality on the growth behavior of the culture. Furthermore, the obtained data in the 300-L pilot-scale reactor fully support the predictive capabilities of the earlier developed small-scale model (Neunstoecklin et al. 2015) and indicate that maximum hydrodynamic stress should be the scaling criteria of choice when agitation is considered as the main source of hydrodynamic stress.

Discussion

Determination of a scale-independent safe operating range by scale-down models is limited, because available published models are not validated using pilot- or manufacture-scale conditions. In this work, a validation of an earlier developed oscillating hydrodynamic stress scale-down model (Neunstoecklin et al. 2015) was discussed using a 300-L pilot-scale bioreactor. Maximum hydrodynamic stress values at this scale were determined at various operating parameters with a shear sensitive particulate system based on the breakage of aggregates composed of polymer nanoparticles (Villiger et al. 2015). The same method was used to characterize the maximum shear stress in the lower scale units, providing coherence to the entire procedure. Using the measured hydrodynamic stress threshold of the investigated Sp2/0 cell line equal to 25 Pa, the operating conditions for the pilot scale were set either well below (7 Pa) or slightly above (28 Pa) this value. The obtained results were compared with our previous data (Neunstoecklin et al. 2015) from either classical 3-L cultivations and with data obtained from the oscillating stress loop system. The growth behavior of the cells at high agitation

was reduced but showed a better longevity expressed through a higher viability at the end of the cultivation (see Fig. 3). Very similar results were obtained from the oscillating hydrodynamic stress loop scale-down model applying comparable hydrodynamic conditions. Furthermore, as shown in Figs. 4c and 5, the productivity and product quality were very much aligned throughout the scales when comparing similar stress values. Although no statistical difference could be shown, a trend to more complex glycosylation forms as well as a shift to more basic charged variants could be observed with increasing stresses beyond the edge of failure, thus being dependent on the hydrodynamic stress value rather than on the actual reactor scale. These results are in agreement with previous works published in literature where only minor effects on quality attributes like glycosylation or charged variant distribution were observed, as long as no changes in the growth behavior or basic metabolites were detected (Senger and Karim 2003; Scott et al. 2012; Sieck et al. 2013; Nienow et al. 2013; Neunstoecklin et al. 2015).

Compared to previous studies of cell response to elevated stresses using various scale-down models (Ma et al. 2002; Nienow 2006; Mollet et al. 2007; Godoy-Silva et al. 2009a, b; Sieck et al. 2013; Nienow et al. 2013), the data presented here shows for the first time a validation study for a scale-down model using an edge of failure approach at pilot scale, thereby proving the applicability and predictability of the corresponding model developed by our group (Neunstoecklin et al. 2015). This assures better confidence when applying it in a quality by design framework, when determining the maximum agitation operating range of a process. Additionally, the maximum stress determination approach considered in this work in combination with the shear characterization is applicable for any kind of system, including single use, not geometrically different systems and non-stirred reactors. It enables better understanding to decide on appropriate mixing conditions than criteria based on power input (P/V) to ensure sufficient gas mass transfer. This can be of specific interest for novel high cell density fed-batch or perfusion cultures.

Acknowledgments The authors would like to acknowledge SNF (200020_147137/1) for financial support of this project. Furthermore, Miroslav Soos was partially supported by the Specific University Research grant of UCT (grant number 20/2015).

Compliance with ethical standards

Funding This study was funded by SNF (grant number 200020_147137/1).

This study was partially funded by the Research grant of UCT (grant number 20/2015).

Conflict of interest Benjamin Neunstoecklin declares that he has no conflict of interest.

Thomas K. Villiger declares that he has no conflict of interest.

Eric Lucas declares that he has no conflict of interest.

Matthieu Stettler declares that he has no conflict of interest.

Hervé Broly declares that he has no conflict of interest.

Massimo Morbidelli declares that he has no conflict of interest.

Miroslav Soos declares that he has no conflict of interest.

Ethical approval This article does not contain any studies with human participants or animals performed by any of the authors.

References

Adams D, Korke R, Hu WW (2007) Application of stoichiometric and kinetic analyses to characterize cell growth and product formation. In: Pörtner R (ed) Animal cell biotechnology—methods and protocols, 2nd edn. Human Press Inc., Totowa, pp 269–284

Al-Rubeai M, Singh RP, Goldman MH, Emery AN (1995) Death mechanisms of animal cells in conditions of intensive agitation. Biotechnol Bioeng 45:463–472. doi:10.1002/bit.260450602

Amanullah A, Nienow AW, Emery AN, McFarlane CM (1993) The use of *Bacillus subtilis* as an oxygen sensitive culture to simulate dissolved oxygen cycling in large scale fermenters. Trans I Chem E Part C:206–208

Berridge J, Seamon K, Venugopal S (2009) A-Mab: a case study in bioprocess development. 1–278

Boulton-Stone JM, Blake JR (1993) Gas bubbles bursting at a free surface. J Fluid Mech 254:437–466

Chalmers JJ, Bavarian F (1991) Microscopic visualization of insect cell-bubble interactions. II: the bubble film and bubble rupture. Biotechnol Prog 7:151–8. doi:10.1021/bp00008a010

Chisti Y (2000) Animal-cell damage in sparged bioreactors. Trends Biotechnol 18:420–432. doi:10.1016/S0167-7799(00)01474-8

Clincke M-F, Guedon E, Yen FT, Ogier V, Roitel O, Goergen J-L (2010) Effect of surfactant pluronic F-68 on *CHO* cell growth, metabolism, production, and glycosylation of human recombinant IFN-γ in mild operating conditions. Biotechnol Prog 27:181–90. doi:10.1002/btpr.503

Croughan MS, Hamel JF, Wang DI (1987) Hydrodynamic effects on animal cells grown in microcarrier cultures. Biotechnol Bioeng 29:130–41. doi:10.1002/bit.260290117

Cruz PE, Cunha A, Peixoto CC, Clemente J, Moreira JL, Carrondo MJ (1998) Optimization of the production of virus-like particles in insect cells. Biotechnol Bioeng 60:408–18

Ehrl L, Soos M, Wu H, Morbidelli M (2010) Effect of flow field heterogeneity in coagulators on aggregate size and structure. AIChE J 56:2573–2587. doi:10.1002/aic.12179

Emery AN, Jan DC, Al-Rubeai M (1995) Oxygenation of intensive cell-culture system. Appl Microbiol Biotechnol 43:1028–33

Flickinger MC (2013) Upstream industrial biotechnology, 2 volume Set. John Wiley & Sons Inc, New York

Gigout A, Buschmann MD, Jolicoeur M (2008) The fate of pluronic F-68 in *chondrocytes* and *CHO* cells. Biotechnol Bioeng 100:975–87. doi:10.1002/bit.21840

Glacken MW, Fleischaker RJ, Sinskey AJ (1983) Mammalian cell culture: engineering principles and scale-up. Trends Biotechnol 1:102–108. doi:10.1016/0167-7799(83)90032-X

Godoy-Silva R, Chalmers JJ, Casnocha S, Bass LA, Ma N (2009a) Physiological responses of *CHO* cells to repetitive hydrodynamic stress. Biotechnol Bioeng 103:1103–17. doi:10.1002/bit.22339

Godoy-Silva R, Mollet M, Chalmers JJ (2009b) Evaluation of the effect of chronic hydrodynamical stresses on cultures of suspensed *CHO-6E6* cells. Biotechnol Bioeng 102:1119–30. doi:10.1002/bit.22146

Handa-Corrigan A, Emery AN, Spier RE (1989) Effect of gas–liquid interfaces on the growth of suspended mammalian cells:

mechanisms of cell damage by bubbles. Enzym Microb Technol 11: 230–235. doi:10.1016/0141-0229(89)90097-5

Hua J, Erickson LE, Yiin TY, Glasgow LA (1993) A review of the effects of shear and interfacial phenomena on cell viability. Crit Rev Biotechnol 13:305–28. doi:10.3109/07388559309075700

Hudcova V, Machon V, Nienow AW (1989) Gas–liquid dispersion with dual rushton turbine impellers. Biotechnol Bioeng 34:617–28. doi:10.1002/bit.260340506

Humphrey A (1998) Shake flask to fermentor: what have we learned? Biotechnol Prog 14:3–7. doi:10.1021/bp970130k

Jöbses I, Martens D, Tramper J (1991) Lethal events during gas sparging in animal cell culture. Biotechnol Bioeng 37:484–90. doi:10.1002/bit.260370510

Jordan M, Eppenberger HM, Sucker H, Widmer F, Einsele A (1994) Interactions between animal cells and gas bubbles: the influence of serum and pluronic F68 on the physical properties of the bubble surface. Biotechnol Bioeng 43:446–54. doi:10.1002/bit.260430603

Ju L-K, Chase GG (1992) Improved scale-up strategies of bioreactors. Bioprocess Eng 8:49–53. doi:10.1007/BF00369263

Kunas KT, Papoutsakis ET (1990) Damage mechanisms of suspended animal cells in agitated bioreactors with and without bubble entrainment. Biotechnol Bioeng 36:476–83. doi:10.1002/bit.260360507

Le H, Kabbur S, Pollastrini L, Sun Z, Mills K, Johnson K, Karypis G, Hu W-S (2012) Multivariate analysis of cell culture bioprocess data—lactate consumption as process indicator. J Biotechnol 162:210–23. doi:10.1016/j.jbiotec.2012.08.021

Leist C, Meyer H-P, Fiechter A (1986) Process control during the suspension culture of a human melanoma cell line in a mechanically stirred loop bioreactor. J Biotechnol 4:235–246. doi:10.1016/0168-1656(86)90028-3

Li F, Hashimura Y, Pendleton R, Harms J, Collins E, Lee B (2006) A systematic approach for scale-down model development and characterization of commercial cell culture processes. Biotechnol Prog 22:696–703. doi:10.1021/bp0504041

Li F, Vijayasankaran N, Shen A (Y), Kiss R, Amanullah A (2010) Cell culture processes for monoclonal antibody production. MAbs 2: 466–479. doi:10.4161/mabs.2.5.12720

Li J, Wong CL, Vijayasankaran N, Hudson T, Amanullah A (2012) Feeding lactate for *CHO* cell culture processes: impact on culture metabolism and performance. Biotechnol Bioeng 109:1173–86. doi:10.1002/bit.24389

Liu Y, Hu W, Wiltberger K, Ryll T, Li F (2013) Effects of bubble-liquid two-phase turbulent hydrodynamics on cell damage in sparged bioreactor. Biotechnol Prog. doi:10.1002/btpr.1790

Ma N, Koelling KW, Chalmers JJ (2002) Fabrication and use of a transient contractional flow device to quantify the sensitivity of mammalian and insect cells to hydrodynamic forces. Biotechnol Bioeng 80:428–37. doi:10.1002/bit.10611

Ma N, Chalmers JJ, Auniņs JG, Zhou W, Xie L (2004) Quantitative studies of cell-bubble interactions and cell damage at different pluronic F-68 and cell concentrations. Biotechnol Prog 20:1183–91. doi:10.1021/bp0342405

Marks DM (2003) Equipment design considerations for large scale cell culture. Cytotechnology 42:21–33. doi:10.1023/A:1026103405618

Meier SJ, Hatton TA, Wang DI (1999) Cell death from bursting bubbles: role of cell attachment to rising bubbles in sparged reactors. Biotechnol Bioeng 62:468–78

Michaels JD, Mallik AK, Papoutsakis ET (1996) Sparging and agitation-induced injury of cultured animals cells: do cell-to-bubble interactions in the bulk liquid injure cells? Biotechnol Bioeng 51:399–409. doi:10.1002/(SICI)1097-0290(19960820)51:4<399::AID-BIT3>3.0.CO;2-D

Mollet M, Godoy-Silva R, Berdugo C, Chalmers JJ (2007) Acute hydrodynamic forces and apoptosis: a complex question. Biotechnol Bioeng 98:772–88. doi:10.1002/bit.21476

Mostafa SS, Gu X (2003) Strategies for improved dCO2 removal in large-scale fed-batch cultures. Biotechnol Prog 19:45–51. doi:10.1021/bp0256263

Murhammer DW, Goochee CF (1990) Sparged animal cell bioreactors: mechanism of cell damage and pluronic F-68 protection. Biotechnol Prog 6:391–7. doi:10.1021/bp00005a012

Murhammer DW, Pfalzgraf EC (1992) Effects of pluronic F-68 on oxygen transport in an agitated, sparged bioreactor. Biotechnol Tech 6: 199–202. doi:10.1007/BF02439343

Neunstoecklin B, Stettler M, Solacroup T, Broly H, Morbidelli M, Soos M (2015) Determination of the maximum operating range of hydrodynamic stress in mammalian cell culture. J Biotechnol 194:100–9. doi:10.1016/j.jbiotec.2014.12.003

Nienow AW (1998) Hydrodynamics of stirred bioreactors. Appl Mech Rev 51:3–32. doi:10.1115/1.3098990

Nienow AW (2006) Reactor engineering in large scale animal cell culture. Cytotechnology 50:9–33. doi:10.1007/s10616-006-9005-8

Nienow AW, Scott WH, Hewitt CJ, Thomas CR, Lewis G, Amanullah A, Kiss R, Meier SJ (2013) Scale-down studies for assessing the impact of different stress parameters on growth and product quality during animal cell culture. Chem Eng Res Des. doi:10.1016/j.cherd.2013.04.002, **1–10**

Oh SKW, Nienow AW, Al-Rubeai M, Emery AN (1989) The effects of agitation intensity with and without continuous sparging on the growth and antibody production of hybridoma cells. J Biotechnol 12:45–61. doi:10.1016/0168-1656(89)90128-4

Oh SKW, Nienow AW, Al-Rubeai M, Emery AN (1992) Further studies of the culture of *mouse hybridomas* in an agitated bioreactor with and without continuous sparging. J Biotechnol 22:245–70

Osman JJ, Birch J, Varley J (2002) The response of *GS-NS0 myeloma* cells to single and multiple pH perturbations. Biotechnol Bioeng 79: 398–407. doi:10.1002/bit.10198

Papac DI, Briggs JB, Chin ET, Jones AJ (1998) A high-throughput microscale method to release N-linked oligosaccharides from glycoproteins for matrix-assisted laser desorption/ionization time-of-flight mass spectrometric analysis. Glycobiology 8:445–54

Paul EL, Atiemo-Obeng VA, Kresta SM (2003) Handbook of industrial mixing. Wiley, Hoboken, NJ, USA

Perry RH, Green DW, Maloney JO (1997) Perry's chemical engineers' handbook, 7th edn. McGraw-Hill, NewYork

Rapp E, Hennig R, Borowiak M, Kottler R, Reichl U (2011) High-throughput glycosylation pattern analysis of glycoproteins utilizing a multiplexing capillary-DNA-sequencer. Glycoconj J 28:234–235

Schmidt FR (2005) Optimization and scale up of industrial fermentation processes. Appl Microbiol Biotechnol 68:425–35. doi:10.1007/s00253-005-0003-0

Scott WH, Thomas CR, Hewitt CJ, Lewis G, Meier SJ, Amanullah A, Kiss R, Nienow AW (2012) Scale-down studies for assessing the impact of different stress parameters on growth and product quality during mammalian cell culture. In: 14th European conference on mixing. Warszawa, pp 431–436

Senger RS, Karim MN (2003) Effect of shear stress on intrinsic *CHO* culture state and glycosylation of recombinant tissue-type plasminogen activator protein. Biotechnol Prog 19:1199–209. doi:10.1021/bp025715f

Serrato JA, Palomares LA, Meneses-Acosta A, Ramírez OT (2004) Heterogeneous conditions in dissolved oxygen affect N-glycosylation but not productivity of a monoclonal antibody in hybridoma cultures. Biotechnol Bioeng 88:176–88. doi:10.1002/bit.20232

Sieblist C, Jenzsch M, Pohlscheidt M (2013) Influence of pluronic(®) F68 on oxygen mass transfer. Biotechnol Prog 29:1278–88. doi:10.1021/btpr.1770

Sieck JB, Cordes T, Budach WE, Rhiel MH, Suemeghy Z, Leist C, Villiger TK, Morbidelli M, Soos M (2013) Development of a scale-down model of hydrodynamic stress to study the performance

of an industrial *CHO* cell line under simulated production scale bioreactor conditions. J Biotechnol 164:41–9. doi:10.1016/j.jbiotec.2012.11.012

Soos M, Moussa AS, Ehrl L, Sefcik J, Wu H, Morbidelli M (2008) Effect of shear rate on aggregate size and morphology investigated under turbulent conditions in stirred tank. J Colloid Interface Sci 319:577–89. doi:10.1016/j.jcis.2007.12.005

Soos M, Kaufmann R, Winteler R, Kroupa M, Lüthi B (2013) Determination of maximum turbulent energy dissipation rate generated by a rushton impeller through large eddy simulation. AIChE J 59:3642–3658. doi:10.1002/aic.14206

Trinh K, Garcia-Briones M, Chalmers JJ, Hink F (1994) Quantification of damage to suspended insect cells as a result of bubble rupture. Biotechnol Bioeng 43:37–45. doi:10.1002/bit.260430106

Villiger TK, Morbidelli M, Soos M (2015) Experimental determination of maximum effective hydrodynamic stress in multiphase flow using shear sensitive aggregates. AIChE J 61:1735–1744. doi:10.1002/aic.14753

Wu J (1995) Mechanisms of animal cell damage associated with gas bubbles and cell protection by medium additives. J Biotechnol 43:81–94

Xing ZZ, Kenty BMN, Li ZJ, Lee SS (2009) Scale-up analysis for a *CHO* cell culture process in large-scale bioreactors. Biotechnol Bioeng 103:733–46. doi:10.1002/bit.22287

Yang J, Lu C, Stasny B, Henley J, Guinto W, Gonzalez C, Gleason J, Fung M, Collopy B, Benjamino M, Gangi J, Hanson M, Ille E (2007) Fed-batch bioreactor process scale-up from 3-L to 2,500-L scale for monoclonal antibody production from cell culture. Biotechnol Bioeng 98:141–54. doi:10.1002/bit.21413

Zagari F, Jordan M, Stettler M, Broly H, Wurm FM (2012) Lactate metabolism shift in *CHO* cell culture: the role of mitochondrial oxidative activity. New Biotechnol. doi:10.1016/j.nbt.2012.05.021

Zhu Y, Cuenca JV, Zhou W, Varma A (2008) *NS0* cell damage by high gas velocity sparging in protein-free and cholesterol-free cultures. Biotechnol Bioeng 101:751–60. doi:10.1002/bit.21950